AJNR

In Utero Eye Development Documented by Fetal MR Imaging

L.B. Paquette, H.A. Jackson, C.J. Tavaré, D.A. Miller and A. Panigrahy

In Utero Eye Development Documented by Fetal MR Imaging

L.B. Paquette
H.A. Jackson
C.J. Tavaré
D.A. Miller
A. Panigrahy

BACKGROUND AND PURPOSE: To date, very limited attention has been given to ocular abnormalities or growth parameters detected by fetal MR imaging. Our objective was to retrospectively determine the relationship between different parameters of eye development and estimated gestational age in the human fetus by use of fetal MR imaging.

MATERIALS AND METHODS: A retrospective study was performed to measure the transverse diameter, interocular distance, and lens diameter of the globes of 127 fetuses who had a morphologically normal central nervous system. Multiple single-shot T2 fast spin-echo images were obtained with a 1.5T magnet by use of contiguous 3-mm intervals in at least 2 orthogonal planes. Loess curves were fitted to explore the relationship between gestational age and each of the 3 measurements of interest. Different models were compared statistically to determine the model of best fit.

RESULTS: For each variable of interest, the "best" model of eye growth was a quadratic function. Specifically, lens growth seems to plateau after 36 weeks of gestation, interocular distance plateaus after 36 weeks of gestation, and globe growth plateaus after 42 weeks of gestation.

CONCLUSIONS: The lens, orbit, and interocular distance growth of the fetus can be demonstrated on fetal MR imaging. All 3 measurements suggest a quadratic model of growth, which indicates slowing of growth toward the end of gestation.

Normal ranges for fetal orbital measurements throughout the second and third trimesters of pregnancy may have the ability to provide valuable prognostic information for fetuses with abnormalities of orbital development. Ultrasonographic identification of microphthalmia was first described in 1985. Since that time, orbital growth curves have been established on the basis of sonography measurements.[1-5] With the development of rapid acquisition MR imaging as a complement to sonography, more precise assessment of the fetal brain, orbit, and facial structures is possible.

The growth charts for fetal lens and globe measurements, and also binocular and interocular distance, have been established by sonography. Other studies have suggested that these sonography-derived growth charts may be applied to measurements derived from MR imaging.[1-5] However, there are technical differences in evaluation of the orbit by sonography and MR imaging. For example, the sonography measurements of binocular and interocular distance are based on bony landmarks that are difficult to see on MR imaging. In addition, certain internal structures within the globes, including the lens, are better differentiated with MR imaging compared with sonography.

Few reports in the literature of the use of fetal MR imaging have documented the growth of the orbit. These studies have limitations, including a small number of subjects and not including measurements of internal structures of the orbit, including the lens. In addition, the previous MR imaging reports have statistical limitations, including assuming linear growth of orbital structures with respect to statistical modeling and lack of statistical confidence intervals to account for variability. Most of the literature on fetal eye growth, based on autopsy, prenatal sonography, and fetal MR imaging measurements, has suggested a linear growth curve.[5-15] Others have suggested an exponential growth pattern.[16-18] Also, Denis et al[19] in 1998 described a quadratic growth pattern on the basis of autopsy measurements.

Our objective was to retrospectively determine the relationship between selected orbital measurements and estimated gestational age in fetal MR imaging studies with a morphologically normal central nervous system (CNS) and orbits for the purpose of creating normal growth curves. We measured 3 variables: transverse globe diameter, transverse lens diameter, and interocular distance. We also used Loess curves and statistical analysis to determine the best statistical fit for an orbital growth model, given the variety of growth curves that have been used to describe fetal growth.

Materials and Methods

Patient Selection

Fetal MR images were reviewed retrospectively in this institutional review board–approved study that was also compliant with the terms of the Health Insurance Portability and Accountability Act. The need to obtain informed consent from the parents was waived. Data from imaging studies of 192 fetuses between January 2002 and January 2005 were available for review. The following inclusion criteria were applied: 1) documented MR imaging report of an anatomically and
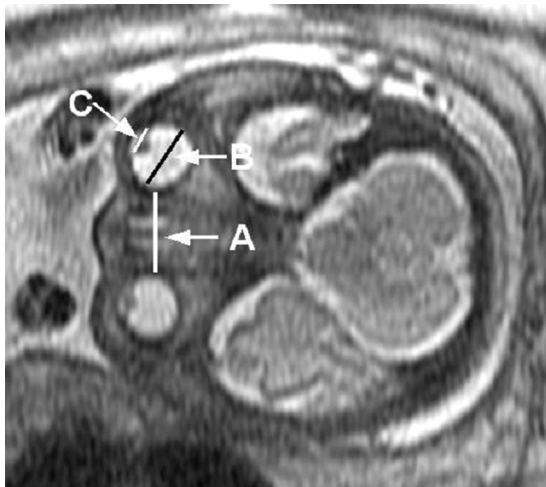
Fig 1. MR imaging of fetal eye measurements. *A*, Interocular measurement. *B*, Globe measurement. *C*, Lens measurement.

developmentally appropriate fetal CNS, and 2) absence of a documented fetal chromosomal abnormality.

A total of 65 MR images were excluded from the original 192 for a CNS and/or orbital anomaly. Of the remaining 127, there were a variety of diagnoses (congenital diaphragmatic hernia, gastroschisis, twins, urologic abnormalities, cystic adenomatoid malformation, etc). Results of 26 MR images in this group were completely normal but had some suspicion on the basis of history and/or prenatal ultrasound examination. Each fetus was measured at 1 time point. All images were reviewed by at least 1 of 2 pediatric neuroradiologists (all of whom had at least 3–4 years of experience with reading fetal MR images) to confirm that the CNS and orbits were morphologically normal. Estimated gestational age was determined on the basis of standard clinical criteria. When available, postnatal medical records and imaging studies were reviewed to confirm normal brain development or ocular development.

MR Imaging Technique

Using a 1.5T magnet, we placed a body coil over the mother's abdomen and obtained multiple single-shot T2 fast spin-echo images using 3 mm (0-mm gap) in at least 2 orthogonal planes. The parameters were TR, 5 to 12 ms; TE, 70 ms; 1 signal intensity acquired; flip angle, 150 to 180°; and matrix, 128 × 320. Quantitative measurements were performed on a PACS (Synapse; Fujifilm Medical Systems, Stamford, Conn). The maximal transverse diameter of the globe and lens were recorded for each eye, as was the interocular distance (Fig 1). These measurements were made in planes that were true axial provided that both eyes were seen in the same image and had transverse diameters that were equal and as large as possible. In a small subset of cases (5%), a true coronal image was used when the axial images were corrupted by fetal motion or were nonorthogonal. Measurements were performed by 1 person to maintain consistency. The transverse diameter of the globe was taken from the malar margin of the vitreous to the ethmoidal margin of the vitreous. The interocular distance was measured between the 2 ethmoidal margins of the vitreous. The lens clearly demonstrates low signal intensity compared with the surrounding hyperintense vitreous fluid. Of note, a small subset of fetuses (total of 12 cases) was excluded because the MR images were degraded by fetal motion, head rotation, and/or off-axis imaging.

Statistical Analysis

No assumptions (linear or exponential) were made with regard to a growth model. Loess curves were made comparing measurements with gestational age to determine which mathematical model best described each measurement's growth pattern.[20] We performed statistical analyses using Minitab Statistical Software (Minitab, State College, Pa). Initially, the Loess curves for mean lens diameter, interocular distance, and mean globe diameter were examined (Figs 2, 3, and 4, respectively). A Loess curve is a smoothed curve drawn through the points on a (x, y) scatterplot.[21] From a fundamental perspective, linear regressions were fitted to dependent data (y-values [eg, measurements]) for small overlapping sections of the independent data (x-values [eg, gestational ages]). Greater weight was given to observations closest to the interval midpoint. For each fitted linear regression, a predicted value for the dependent y-variable was made for the midpoint of the x-axis interval. A Loess curve is the curve drawn through the predicted y-values.

Results

Developmental Changes in Eye Measurements

For 127 healthy fetuses, gestational age ranged from 17 to 39 weeks (Table 1). Most images were obtained at 34 to 35 weeks of gestation. There was another, smaller peak of imaging frequency at 25 weeks of gestation. Differences in left and right eye measurements were not significant for globe ($P > .7$) and lens ($P > .6$) diameters (paired t tests). The average diameter of the left and right eye measurements was used to model the growth of the globe and lens. During the observed 22 weeks of gestation, the increases in measurements approximately were twofold for average lens and globe diameters and interocular distance (Table 2). All 3 Loess curves, for mean left and right globe diameter, mean left and right lens diameter, and interocular distance, suggested a quadratic model.

Determination of Growth Curves by Fitting Techniques

This "best" quadratic fit for each variable was confirmed when the fits to linear and quadratic models were compared (Figs 2, 3, and 4, respectively). The improvement in fit of a quadratic model vs a linear model was highly significant for all 3 measurements: $P = .0004$, $P = .00005$, and $P = .00008$ for average lens diameter, interocular distance, and average globe diameter, respectively. The amount of variation explained by quadratic models was greater than that for exponential models for each measurement. Estimated maximal growth measurements were reached at 36, 36, and 42 weeks of gestation for average lens diameter, interocular distance, and average globe diameter, respectively.

Discussion

Our study has demonstrated that MR imaging is a useful way to obtain measurements of the lens and orbits between 17 and 39 weeks of gestation. These measurements may prove to be useful in the evaluation of the fetus with eye abnormalities. These measurements are easy to obtain from a single plane and can be performed while rendering clinical interpretation of the imaging study. These growth curves, obtained without assumptions of modeling of growth, may be used for clinical application. However, multiple methodologic issues may have affected the accuracy of our results. For example, although
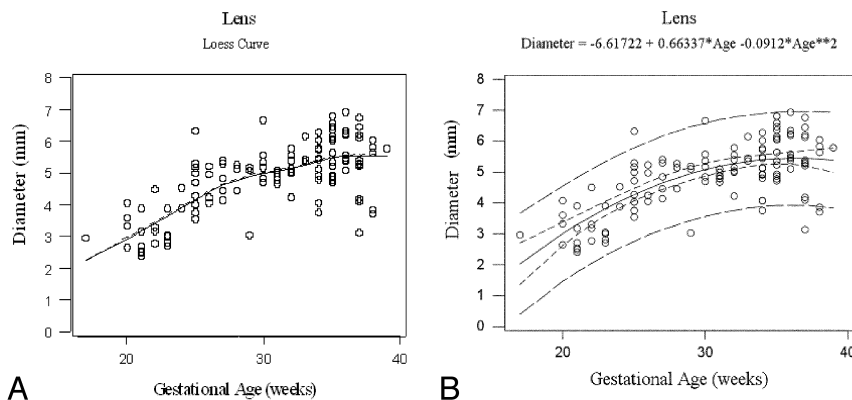
Fig 2. Gestational age vs lens growth. Loess curve for gestational age vs lens growth (*A*). Gestational age vs lens growth with quadratic model. *R*-Square = 0.514, narrow band: 95% confidence interval, wide band: 95% prediction interval (*B*).
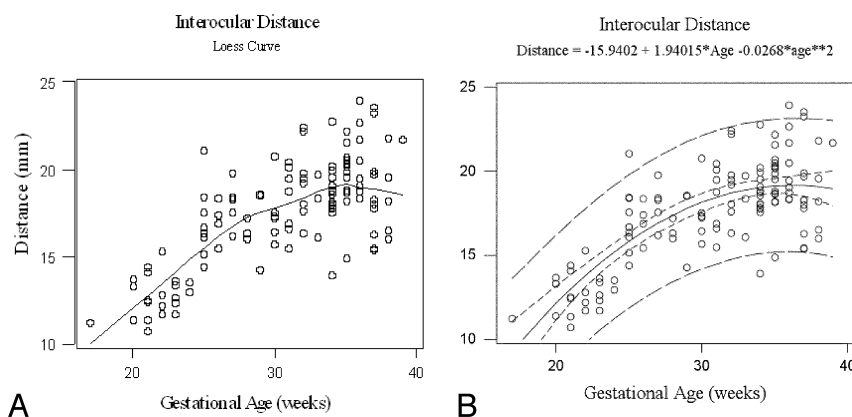

Fig 3. Gestational age vs interocular distance. Loess curve for interocular distance growth vs gestational age (*A*). Gestational age vs interocular distance with quadratic model. *R*-Square = 0.56, narrow band: 95% confidence interval, wide band: 95% prediction interval (*B*).
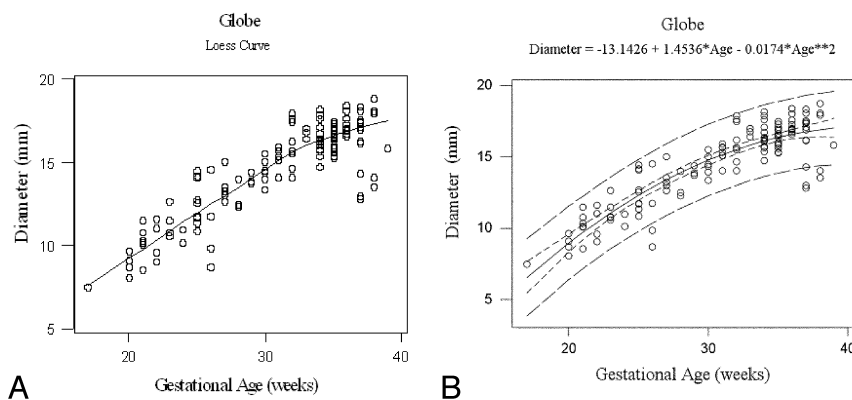

Fig 4. Gestational age vs globe diameter. Loess curve for gestational age vs globe diameter growth (*A*). Gestational age vs globe diameter with quadratic model. *R*-Square = 0.797, narrow band: 95% confidence interval, wide band: 95% prediction interval (*B*).

measurements were performed in patients with no definite CNS abnormality, there still could be a CNS or orbital abnormality that was subtle. In addition, our sample size was limited with a lack of data points, especially in early and late gestation. Also, the gestational dating of the fetuses is not usually exact.

Most of the previous work of fetal eye development has also been described by prenatal sonography and gross anatomic studies of orbits. The eye begins to develop at approximately 22 days of fetal life when 2 indentations (the optic pits) on the primitive forebrain form. These regions grow anteriorly away from the forebrain but remain attached via the optic stalks.

Once this has occurred, the eye primordia are referred to as optic vesicles. The optic vesicles then begin to invaginate and form optic cups. This process is complete by 28 days of fetal life. The contents of the globe then enter into the optic cup by 42 days. During this time the lens has started to develop and the remaining eye structures subsequently differentiate. There is rapid growth of the fetal eye during the eighth to fourteenth weeks of fetal life, and as fetal body growth slows after 30 weeks, so does the fetal eye.[22,23] The molecular controls over fetal eye development are not completely elucidated. Recently, genetic studies have identified a transcription factor, paired

Table 1: Statistics for globe, lens, interocular measurements, and gestational age

	Mean (SD)	Median	Median Range (mm)	P value
Globe diameter				.74
Left eye	14.433 (2.792)	15.225	7.20–18.81	
Right eye	14.458 (2.836)	14.905	7.53–18.75	
Lens diameter				.64
Left eye	4.867 (1.086)	5.070	2.25–7.50	
Right eye	4.854 (1.107)	5.025	2.30–7.03	
Interocular distance	17.504 (2.964)	18.040	10.70–23.95	
Gestational age (weeks)	30.555 (5.577)	32	17–39	

Table 2: Measurements by gestational age

Gestational age (weeks)	n	Lens Diameter* Mean (mm)	SD	Interocular Distance Mean (mm)	SD	Globe Diameter* Mean (mm)	SD
17	1	2.95	.00	11.20	.00	7.45	.00
18	0	—	—	—	—	—	—
19	0	—	—	—	—	—	—
20	4	3.41	.60	12.90	1.03	8.85	.66
21	6	2.87	.58	12.56	1.46	10.21	.98
22	4	3.44	.74	12.97	1.58	10.31	1.20
23	5	3.09	.48	12.71	.79	11.24	.85
24	2	4.21	.45	13.23	.40	10.53	.60
25	10	4.62	.85	17.08	1.90	12.48	1.33
26	4	4.63	.57	17.02	1.23	11.20	2.56
27	5	4.83	.55	18.04	1.31	13.49	.91
28	3	4.96	.43	16.50	.62	12.93	.94
29	3	4.44	1.22	17.12	2.46	14.00	.35
30	6	5.39	.71	17.49	1.74	14.46	.77
31	7	4.88	.14	18.25	1.94	15.27	.62
32	8	5.14	.48	19.38	2.14	16.14	1.43
33	3	5.66	.44	18.06	1.85	16.74	.30
34	14	5.11	.75	18.63	1.92	16.45	.97
35	15	5.72	.71	19.50	1.75	16.39	.70
36	9	5.86	.60	20.30	2.04	17.28	.62
37	12	5.29	1.06	18.44	2.80	16.27	1.90
38	5	5.02	1.14	18.42	2.36	16.49	2.48
39	1	5.79	.00	21.71	.00	15.84	.00

* Average of left and right eye measurements.

box gene 6, or *PAX6*, which seems to be a master control gene for eye development.[23,24] Mutations in this gene have been associated with aniridia and optic nerve abnormalities.

We did find that a quadratic model best fits fetal eye growth with regard to the fetal MR imaging measurements in this study. Most ultrasonographic and postmortem autopsy studies have described a linear pattern of fetal eye and eye structure growth.[5-13] A few authors have suggested that exponential models of growth better suit the fetal eye, including the curve model by Jeanty et al,[17] which seem to be used most by obstetricians.[16,17] Many other studies in the literature were fitted to a linear growth curve, including another fetal MR imaging study.[5,10,13,15] The others were fitted to lower-order polynomials.[16,17] These studies used statistical methods that assume linear or exponential modeling of growth.

A study by Denis et al,[19] which suggests a quadratic model best fits fetal eye growth, supports our results. In their study, pathologic specimens were measured with calipers and were not fitted to a certain curve shape. The correlation between gross anatomic examination and fetal MR imaging measure-ments gives strength to the validity of our measurements. The quadratic model suggests a slowing of fetal eye growth toward the end of gestation, the mechanism of which is unknown. Fledelius and Christensen[16] suggested that the fetal eye axial growth seems to decelerate with time. This pattern seems to parallel the head circumference growth seen in the fetus and preterm neonates.[7,25,26]

We found distinct differences between our study and other fetal MR imaging studies of eye development according to the type of measurements performed and statistical modeling. The study by Bremond-Gignac et al[15] included 35 fetuses from 20 to 40 weeks of gestation and measured the ocular surface area. Their results suggested a linear model of growth for the fetal eye. Robinson et al[18] published fetal MR imaging eye growth curves on the basis of a logarithmic regression model with 111 healthy fetuses. They measured interocular distance and binocular distance, and calculated the orbital diameter. It is noteworthy that their interocular distance values were greater than ours and their orbital diameter values were overall smaller than ours. In addition, the decrease in orbital diameter seen toward the end of gestation in our data was not demon-strated by theirs. Our study had a greater distribution of pa-tients in this age group vs theirs. Similar to their findings, our measurements yielded smaller values compared with the es-tablished sonography curves, likely because of enhanced accu-racy as MR imaging enables visualization of soft tissue, not just bony structures as seen on sonography. Ying et al[14] recently evaluated fetal eye growth by MR imaging in 27 subjects at 21 to 37 weeks of gestational age. They measured the anteropos-terior length of the eye and the transverse diameter. Their transverse diameter measurements differed from ours in that they measured from the lateral border of the eye (zygomatic bone) to the median nasal septum, not the medial border of the orbit. Their measurements suggested that the transverse diameter growth continues to increase to term, but they did not try to plot their points on a growth curve. It is interesting to note that they also found their anteroposterior measure-ments decreased after 28 weeks of gestation. We did not exam-ine the anteroposterior diameter, but our orbital diameter measurements follow this trend. To our knowledge, no previ-ous fetal MR imaging studies have looked at lens growth. Achi-ron et al[9] in 1995 reported a linear growth pattern of the fetal lens circumference based on fetal sonography measurements. Goldstein et al[10] and Dilmen et al[13] described linear growth of the fetal lens diameter by prenatal sonography measurements.

Our lens, orbit, and interocular distance growth curves es-tablish fetal eye growth norms as seen on MR imaging and may be helpful in identifying abnormal eyes in the fetus. Microph-thalmia is defined as macroscopic absence of the eye with the presence of histologic eye remnants,[27] and the condition is estimated to occur in 1 in 5000 to 1 in 8300 live births and 1 in 2400 pregnancies.[1,2] The condition may be unilateral or bilat-eral. The causes of microphthalmia are many, including other chromosomal abnormalities, craniofacial disorders, intra-uterine infections (toxoplasmosis, varicella, rubella, parvovi-rus B19, influenza, cytomegalovirus, herpes, Epstein-Barr vi-rus, syphilis),[28-34] possible teratogens (ethanol, herbicides, retinoic acid, isotretinoin, cyclophosphamide, heavy metals, hyperthermia, radiation, vitamin A deficiency, maternal phe-nylketonuria),[33,35-39] and multiple syndromes (>180 listed on

On-line Mendelian Inheritance in Man data base[40]). Therefore, associated anomalies are common and may include the following (in decreasing order of frequency): other eye abnormalities (coloboma, congenital cataract), ear anomalies, limb abnormalities (upper and lower limb), brain abnormalities, skull/face/jaw anomalies, abnormal nails, atrial septal defects, and genital abnormalities.[22,24] It has been accepted that microphthalmia can be diagnosed early in pregnancy because the abnormal development has occurred by 7 weeks of fetal life; however, Blazer et al[1] describe a few patients with microphthalmia who had normal fetal eyes on sonography results at up to 27 weeks of gestation. The CEH-10 homeobox-containing homolog gene, *CHX10* or *HOX10,* on chromosome 14 is associated with isolated microphthalmia of the type called *MCOP2. MCOP1*, another isolated microphthalmia form, maps to a different location on the same chromosome, and the gene is not known but the inheritance is the same—autosomal recessive (On-line Mendelian Inheritance in Man).[40] There are additional forms of microphthalmia associated with other ocular or nonocular abnormalities.

Our lens, orbit, and interocular distance growth curves establish fetal eye growth norms as seen on MR imaging and may be helpful to identify cases of microphthalmia in the fetus.[41] With these normal growth parameters as a reference, our future work will include determining if our growth curves enable detection of additional fetal eye and/or brain anomalies by MR imaging. Other future work is aimed at studying other parameters of eye development (surface areas, volume, signal intensity, hydrographic imaging). Improvements in fast MR imaging techniques will also help acquire thinner sections of the globe, which will facilitate obtaining accurate volumetric measurement.

Conclusions

The lens, orbit, and interocular distance growth of the fetus has been measured by fetal MR imaging. All 3 measurements suggest a quadratic model of growth, which indicates slowing of growth toward the end of gestation.

References

1. Blazer S, Zimmer E, Mezer E, et al. **Early and late onset fetal microphthalmia.** *Am J Obstet Gynecol* 2006;194:1354–59
2. Twining P. **Abnormalities of the face and neck.** In: Twining P, McHugo JM, Pilling DW, eds. *Textbook of Fetal Abnormalities.* London: Churchill Livingstone; 2000:345–88
3. Trout T, Budorick N, Pretorius D, et al. **Significance of orbital measurements in the fetus.** *J Ultrasound Med* 1994;13:937–43
4. Mayden K, Tortora M, Berkowitz R, et al. **Orbital diameters: a new parameter for prenatal diagnosis and dating.** *Am J Obstet Gynecol* 1982;144:289–98
5. Birnholz JC. **Ultrasonic fetal ophthalmology.** *Early Hum Dev* 1985;12:199–209
6. Achiron R, Kreiser D, Achiron A. **Axial growth of the fetal eye and evaluation of the hyaloid artery: in utero ultrasonographic study.** *Prenat Diagn* 2000;20:894–99
7. Denis D, Righini M, Scheiner C, et al. **Ocular growth in the fetus. 1. Comparative study of axial length and biometric parameters in the fetus.** *Ophthalmologica* 1993;207:117–24
8. Harayama K, Amemiya T, Nishimura H. **Development of the eyeball during fetal life.** *J Pediatr Ophthalmol Strabismus* 1981;18:37–40
9. Achiron R, Gottlieb Z, Yaron Y, et al. **The development of the fetal eye: in utero ultrasonographic measurements of the vitreous and lens.** *Prenat Diagn* 1995;15:155–60
10. Goldstein I, Tamir A, Zimmer EZ, et al. **Growth of the fetal orbit and lens in normal pregnancies.** *Ultrasound Obstet Gynecol* 1998;12:175–79
11. Sivan Y, Merlob P, Reisner SH. **Eye measurements in preterm and term newborn infants.** *J Craniofac Genet Dev Biol* 1982;2:239–42
12. Isenberg SJ, Neumann D, Cheong PY, et al. **Growth of the internal and external eye in term and preterm infants.** *Ophthalmology* 1995;102:827–30
13. Dilmen G, Koktener A, Turhan NO, et al. **Growth of the fetal lens and orbit.** *Int J Gynaecol Obstet* 2002;76:267–71
14. Ying X, Li H, Yew DT. **Morphometric measurements of fetal and neonatal eyes using MRI and ultrasound.** *Neuroembryol Aging* 2008;5:60–62
15. Bremond-Gignac DS, Benali K, Deplus S, et al. **In utero eyeball development study by magnetic resonance imaging.** *Surg Radiol Anat* 1997;19:319–22
16. Fledelius HC, Christensen AC. **Reappraisal of the human ocular growth curve in fetal life, infancy, and early childhood.** *Br J Ophthalmol* 1996;80:918–21
17. Jeanty P, Dramaix-Wilmet M, Van Gansbeke D, et al. **Fetal ocular biometry by ultrasound.** *Radiology* 1982;143:513–16
18. Robinson AJ, Blaser S, Toi A, et al. **MRI of the fetal eyes: morphologic and biometric assessment for abnormal development with ultrasonographic and clinicopathologic correlation.** *Pediatr Radiol* 2008;38:971–81
19. Denis D, Burguiere O, Burillon C. **A biometric study of the eye, orbit, and face in 205 normal human fetuses.** *Invest Ophthalmol Vis Sci* 1998;39:2232–38
20. R Development Core Team. **R: A Language and Environment for Statistical Computing.** *R Foundation for Statistical Computing.* Vienna, Austria; 2008. Available at: http://www.R-project.org.
21. Venables WN, Ripley BD. *Statistics and Computing: Modern Applied Statistics with S,* 4th ed. New York: Springer-Verlag; 2002:230
22. Edward D, Kaufman L. **Anatomy, development, and physiology of the visual system.** *Pediatr Clin North Am* 2003;50:1–23
23. Graw J. **The genetic and molecular basis of congenital eye defects.** *Nature* 2003;4:876–88
24. Levin A. **Congenital eye anomalies.** *Pediatr Clin North Am* 2003;50:55–76
25. Fenton TR. **A new growth chart for preterm babies: Babson and Benda's chart updated with recent data and a new format.** *BMC Pediatr* 2003;3:13
26. Hadlock FP, Deter RL, Harrist RB, et al. **Fetal head circumference: relation to menstrual age.** *AJR Am J Roentgenol* 1982;138:649–53
27. Shaw G, Carmichael S, Yang W, et al. **Epidemiologic characteristics of anophthalmia and bilateral microphthalmia among 2.5 million births in California, 1989–1997.** *Am J Med Genet A* 2005;135A:36–40
28. Meenken C, Assies J, van Nieuwenhuizen O, et al. **Long term ocular and neurological involvement in severe congenital toxoplasmosis.** *Br J Ophthalmol* 1995;79:581–84
29. Palano G, Di Pietro M, Scuderi A, et al. **Microphthalmia due to congenital varicella infection: a case report.** *Minerva Pediatr* 2005;57:433–39
30. Busby A, Dolk H, Armstrong B. **Eye anomalies: seasonal variation and maternal viral infections.** *Epidemiology* 2005;16:317–22
31. McCarthy R, Frenkel L, Kollarits C, et al. **Clinical anophthalmia associated with congenital cytomegalovirus infection.** *Am J Ophthalmol* 1980;90:558–61
32. Hutto C, Arvin A, Jacobs R, et al. **Intrauterine herpes simplex virus infections.** *J Pediatr* 1987;110:97–101
33. Traboulsi E. **Eye.** In: Stevenson R, Hall J, eds. *Human Malformations and Related Anomalies,* 2nd ed. Oxford University Press; 2006:300–02
34. Navas R, Parra R, Pacheco M, et al. **Congenital bilateral microphthalmos after gestational syphilis.** *Indian J Pediatr* 2006;73:935–36
35. Iyer P, Gammon D, Gee J, et al. **Characterization of maternal influence on teratogenicity: an assessment of developmental toxicity studies for the herbicide cyanazine.** *Regul Toxicol Pharmacol* 1999;29:88–95
36. Ozeki H, Shirai S. **Developmental eye abnormalities in mouse fetuses induced by retinoic acid.** *Jpn J Ophthalmol* 1998;42:162–67
37. Peiffer R, McCullen R, Alles A, et al. **Relationship of cell death to cyclophosphamide-induced ocular malformations.** *Teratog Carcinog Mutagen* 1991;11:203–12
38. Gilani S, Alibhai Y. **Teratogenicity of metals to chick embryos.** *J Toxicol Environ Health A* 1990;30:23–31
39. Edwards M. **Hyperthermia as a teratogen: a review of experimental studies and their clinical significance.** *Teratog Carcinog Mutagen* 1986;6:563–82
40. OMIM - Online Mendelian Inheritance in Man. Available at: http://www.ncbi.nlm.nih.gov/sites/entrez?db=omim
41. Paquette L, Randolph L, Incerpi M, et al. **Fetal microphthalmia diagnosed by magnetic resonance imaging.** *Fetal Diagn Ther* 2008;24:182–85